

# 1 **Genome analysis reveals evolutionary mechanisms of adaptation in systemic dimorphic fungi**

2

3 José F. Muñoz<sup>1</sup>, Juan G. McEwen<sup>2,3</sup>, Oliver K. Clay<sup>3,4</sup>, Christina A. Cuomo<sup>1\*</sup>

4

5 <sup>1</sup>Broad Institute of MIT and Harvard, Cambridge, MA, United States.

6 <sup>2</sup>Cellular and Molecular Biology Unit, Corporación para Investigaciones Biológicas, Medellín, Colombia.

7 <sup>3</sup>School of Medicine, Universidad de Antioquia, Medellín, Colombia.

8 <sup>4</sup>School of Medicine and Health Sciences, Universidad del Rosario, Bogotá, Colombia

9 \* [cuomo@broadinstitute.org](mailto:cuomo@broadinstitute.org)

10

11 **Key Words:** Dimorphic fungi, comparative genomics, virulence evolution, Ajellomycetaceae

12

## 13 **ABSTRACT**

14 Dimorphic fungal pathogens cause a significant human disease burden and unlike most fungal  
15 pathogens affect immunocompetent hosts. To examine the origin of virulence of these fungal  
16 pathogens, we compared genomes of classic systemic, opportunistic, and non-pathogenic species,  
17 including *Emmonsia* and two basal branching, non-pathogenic species in the Ajellomycetaceae,  
18 *Helicocarpus griseus* and *Polytolypa hystricis*. We found that gene families related to plant degradation,  
19 secondary metabolites synthesis, and amino acid and lipid metabolism are retained in *H. griseus* and *P.*  
20 *hystricis*. While genes involved in the virulence of dimorphic pathogenic fungi are conserved in  
21 saprophytes, changes in the copy number of proteases, kinases and transcription factors in systemic  
22 dimorphic relative to non-dimorphic species may have aided the evolution of specialized gene  
23 regulatory programs to rapidly adapt to higher temperatures and new nutritional environments. Notably,  
24 both of the basal branching, non-pathogenic species appear homothallic, with both mating type locus  
25 idiomorphs fused at a single locus, whereas all related pathogenic species are heterothallic. These  
26 differences revealed that independent changes in nutrient acquisition capacity have occurred in the  
27 Onygenaceae and Ajellomycetaceae, and underlie how the dimorphic pathogens have adapted to the  
28 human host and decreased their capacity for growth in environmental niches.

29

## 30 INTRODUCTION

31 Among millions of ubiquitous fungal species that pose no threat to humans, a small number of  
32 species cause devastating diseases in immunocompetent individuals. Notably, many human  
33 pathogenic species are ascomycetes in the order Onygenales, which comprises dermatophytes (e.g.  
34 *Trichophyton* spp.), the spherule-forming dimorphic pathogen *Coccidioides*, and yeast-forming  
35 dimorphic pathogens *Histoplasma*, *Paracoccidioides*, and *Blastomyces*. Dimorphism is a specialized  
36 morphogenetic adaptation allowing both growth in the environment and colonization of a host and is  
37 critical for the lifecycle of dimorphic fungal pathogens <sup>1</sup>. In yeast-forming pathogens, dimorphism has  
38 been broadly defined as the ability to generate both yeast (e.g. blastoconidia) in the host or at 37 °C,  
39 and mycelia (e.g. conidia-producing or other hyphae) in the environment <sup>1</sup>. During fungal evolution,  
40 dimorphism has arisen independently multiple times in saprophytic fungi, as is manifested in the wide  
41 distribution of dimorphic species across the Ascomycota, Basidiomycota and Zygomycota phyla <sup>2</sup>.  
42 Notably, the dimorphic fungi in the order Onygenales are primary pathogens causing systemic mycosis  
43 in healthy humans, and collectively cause over 650,000 new infections a year in the United States  
44 alone <sup>3</sup>. Dimorphic fungi can persist as latent infections in tens of millions of people worldwide and may  
45 reactivate when the host becomes immune-deficient; symptoms of active infection include pneumonia,  
46 acute respiratory distress syndrome, and disseminated disease, which can affect multiple organ  
47 systems <sup>1</sup>.

48

49

50 The largest cluster of thermally dimorphic human pathogenic fungi belongs to the onygenalean family  
51 Ajellomycetaceae, which includes *Histoplasma*, *Paracoccidioides*, and *Blastomyces*. In addition to  
52 these medically important genera, the Ajellomycetaceae family also includes more rarely observed  
53 pathogenic species including *Emmonsia parva* and *Ea. crescens*, which undergo a thermal dimorphic  
54 transition to produce adiaspores rather than yeast and cause adiospiromycosis sporadically in humans  
55 <sup>4,5</sup>. This group also includes *Lacazia loboi*, the yeast-like etiological agent of lobomycosis <sup>6</sup>. Of public  
56 health concern, recent reports have documented the worldwide emergence of yeast-forming  
57 Ajellomycetaceae that cause systemic mycoses predominantly in immunocompromised patients, often  
58 with high case-fatality rates <sup>7,8</sup>. Morphological and phylogenetic analyses were combined to demarcate  
59 species boundaries within the Ajellomycetaceae with clinical significance, which led to a proposed  
60 revision of the taxonomy; this included addition of the new genus *Emergomyces*, which includes the  
61 new species *Es. africanus* and *Es. orientalis*, the description of the new species *Blastomyces*  
62 *percursus*, and ongoing efforts to define additional *Emmonsia*-like and *Blastomyces*-like species <sup>8-10</sup>.

63 Dimorphic species within the Ajellomycetaceae are typically restricted to specific ecological niches and  
64 geographical regions. For example, while *H. capsulatum* and *Es. pasteurianus* are considered to have  
65 worldwide distribution, *B. dermatitidis*, *P. brasiliensis*, and *Es. africanus* are restricted to North America,  
66 Latin America and South Africa, respectively. Non-dimorphic species have also been documented as  
67 early diverging Ajellomycetaceae, including *Emmonsiiellopsis*, *Helicocarpus griseus* and *Polytolypa*  
68 *hystricis*, neither of which has been associated with disease in mammals. These species are found in  
69 environmental samples and do not appear to undergo a thermally regulated dimorphic transition<sup>11–13</sup>.

70

71 We hypothesized that such phenotypic differences within the Ajellomycetaceae could be associated  
72 with gene family expansions or contractions, as a consequence of gene duplication and gene loss  
73 events, and that species comparison might reveal evolutionary mechanisms of adaptation in the  
74 systemic dimorphic fungi. Previous comparative and population genomic studies within  
75 Ajellomycetaceae had found evidence of gene family contractions and expansions associated with  
76 virulence<sup>5,14,15</sup>. Other Onygenales genera outside the Ajellomycetaceae represented by published  
77 genome sequences include *Coccidioides* and the non-pathogenic related species *Uncinocarpus reesii*  
78<sup>16,17</sup>, as well as diverse dermatophytes that cause skin infections<sup>18,19</sup>. Recently, the genomes of four  
79 non-pathogenic Onygenaceae species closely related to *Coccidioides* were described, providing  
80 additional resolution into changes in gene content between pathogenic and non-pathogenic  
81 Onygenales<sup>20</sup>. Together these studies helped establish how gene content is related to the life cycle of  
82 different dimorphic pathogenic fungi and dermatophytes; for example, gene family contractions in  
83 cellulases and other plant metabolism genes, and gene family expansions in proteases, keratinases  
84 and other animal tissue metabolism genes, indicated that dimorphic fungi switched from a nutrition  
85 system based on plants to a system based on animals, though mostly relative to outgroups to the  
86 Onygenales such as *Aspergillus*<sup>14,17–19</sup>. In the Onygenales, this hypothesis was tested experimentally;  
87 comparing growth on a wide variety of compounds revealed that in *Uncinocarpus reesii* hyphal growth  
88 was restricted on carbohydrates and considerably improved on proteins<sup>14</sup>.

89

90 To examine key transition points in evolution of virulence and host adaptation in the dimorphic fungi, we  
91 increased the phylogenetic density within the Ajellomycetaceae by sequencing the genomes of non-  
92 pathogenic and emerging species and then performed comparative genomic analyses of the systemic,  
93 opportunistic, and non-pathogenic species. Although representative genomes for most of the described  
94 pathogenic Onygenales genera have been sequenced, the only strictly non-pathogenic species that  
95 have been sequenced are closely related to *Coccidioides* in the family Onygenaceae. Here, we have

96 sequenced four additional Onygenales species from the family Ajellomycetaceae; this includes *H.*  
97 *griseus* and *P. hystricis*, neither of which has been associated with disease in mammals, and two  
98 additional adiaspore-forming strains of *Ea. parva* and *Ea. crescens* with distinct phenotypic properties.  
99 Leveraging our previous genomic studies and these additional genome sequences, we have  
100 characterized the extent of gene family expansions and contractions to provide a better understanding  
101 of the evolutionary mechanisms of adaptation in systemic dimorphic fungi in the Ajellomycetaceae.

102

103

## 104 RESULTS

105

### 106 Genome comparisons of Ajellomycetaceae, the largest group of dimorphic human pathogenic 107 fungi

108 Building on previous genomic analyses of the members from the Ajellomycetaceae<sup>5,9,14,15,21</sup>, we  
109 sequenced using Illumina technology the genomes of four species within Ajellomycetaceae with  
110 demarcated phenotypic differences. In addition to *Emmonsia parva* UAMH139 and *Emmonsia crescens*  
111 UAMH3008, we sequenced the genomes of one strain of *Emmonsia parva* UAMH130 (type strain) and  
112 one additional strain of *E. crescens* UAMH4076. *E. parva* UAMH130 is from lungs of a rodent in USA,  
113 and *E. crescens* UAMH4076 (type strain) is from a greenhouse source in Canada<sup>22</sup>. We also  
114 sequenced two species that live in soil, where they are found in animal excrement but not associated  
115 with disease; neither species appears to undergo a thermal dimorphic switch to a pathogenic phase, as  
116 there is no observation of a yeast-like form<sup>13,22</sup>. This includes one strain of *Helicocarpus griseus*,  
117 UAMH5409 (type strain; synonym *Spiromastix grisea*), isolated from gazelle dung in Algeria, and one  
118 strain of *Polytolypa hystricis*, UAMH7299, isolated from porcupine dung in Canada.

119

120 The *de novo* genome assemblies of these four species have similar sizes to those of other genera  
121 within the Ajellomycetaceae including *Histoplasma*, *Emergomyces* and *Paracoccidioides*<sup>5,9,14,15</sup>, and  
122 have high representation of conserved eukaryotic genes (**Figure S1, S2**). The assembly sizes were  
123 27.8 Mb in *E. parva* UAMH130, 33.8 Mb in *E. crescens* UAMH4076, 32.0 Mb in *P. hystricis*, and 34.7  
124 Mb in *H. griseus* (**Table 1**). In addition, using both the CEGMA<sup>23</sup> and BUSCO<sup>24</sup> conserved eukaryotic  
125 gene sets, we found that the predicted genes for each sequenced species are nearly complete; all of  
126 these genomes include 96-98% of the core genes (**Figure S2**). The total numbers of predicted genes in  
127 *E. parva* UAMH130 ( $n = 8,202$ ), and *E. crescens* UAMH4076 ( $n = 8,909$ ) were similar to those found in  
128 annotated genome assemblies of other Ajellomycetaceae ( $n = 9,041$  on average); however, relative to

129 other Ajellomycetaceae *P. hystricis*, and *H. griseus* have a modest increase in gene content ( $n = 9,935$   
130 and  $n = 10,225$ , respectively; **Table 1**; **Figure S1**).

131

132 Examining the guanine-cytosine (GC) content in the genomes *E. parva* UAMH130, *E. crescens*  
133 UAMH4076, *H. griseus* UAMH5409 and *P. hystricis* UAMH7299 revealed that none of these genome  
134 assemblies showed evidence of the pronounced bimodality of GC-content observed in *B. gilchristii* and  
135 *B. dermatitidis* (**Figure S3**; **Table 1**; <sup>5</sup>). This highlights that the acquisition of repetitive elements  
136 contributing to bimodal GC distribution were a unique phenomenon during the evolution of the *B.*  
137 *gilchristii* and *B. dermatitidis* within the Onygenales. In addition, UAMH139 showed a small peak of low  
138 GC that is largely absent in UAHM130 (44.4% and 47.5% GC, respectively; **Table 1**), which is  
139 consistent with the phylogenetic divergence between these two strains, and highlights an independent  
140 gain of repetitive sequences (10.4% and 2.6% repetitive bases in UAMH139 and UAMH130,  
141 respectively; **Table 1**). Similarly, *E. crescens* UAMH3008 and UAHM4076 have demarcated differences  
142 in GC and repetitive content; UAHM4076 has a higher peak of low GC sequences (42.9% GC, 15.0%  
143 repetitive bases in UAMH4076; 45.2% GC, 5.1% repetitive bases in UAMH3008; **Table 1**). Additionally,  
144 the more basal strain *P. hystricis* UAMH7299 has a representation of low GC sequences (45.6% GC,  
145 12.8% repeat), but in *H. griseus* UAMH5409 they are almost absent (48.0% GC, 1.8% repeats; **Figure**  
146 **S3**). These results highlight the independent expansion of repetitive elements during Ajellomycetaceae  
147 evolution.

148

#### 149 **Phylogenomic analysis revealed multiple transitions within dimorphic pathogens to enable** 150 **human infection**

151 We estimated a strongly supported phylogeny of the newly sequenced *E. parva* UAMH130, *E.*  
152 *crescens* UAMH4075, *H. griseus* and *P. hystricis* strains relative to other dimorphic fungi using  
153 maximum likelihood and 2,505 single copy core genes (**Figure 1**). Branch length and topology  
154 supported the placement and relationships of *P. hystricis* and *H. griseus* within the Ajellomycetaceae as  
155 basally branching. The two *E. parva* isolates (UAMH130 and UAMH139) do not form a single well-  
156 defined clade, confirming that *E. parva* may not be a single species. In addition to longer branch  
157 lengths suggesting higher divergence of these isolates, the average genome-wide identity between  
158 UAMH130 and UAMH139 is much lower even comparing across groups that represent recently  
159 subdivided species, for example, within *B. gilchristii* and *B. dermatitidis* or *P. lutzii* and *P. brasiliensis*,  
160 with an average identity of 88.6% versus 95.8% and 91.1% respectively (**Figure S4**). *E. parva* (type  
161 strain UAMH130) is the most basal member of the clade including *E. parva* UAMH139 and

162 *Blastomyces* species *B. percursus*, *B. gilchristii*, and *B. dermatitidis*. Previous molecular approaches  
163 <sup>12,25</sup> and recent multi-locus approaches <sup>8,9</sup> also support the polyphyletic nature of *E. parva* isolates.  
164 Although both isolates of *E. crescens* (UAMH3008 and UAMH4076) form a single clade, the genetic  
165 variation between them is also greater than that observed within other species from the same genus in  
166 the Ajellomycetaceae, with long branch lengths and slightly lower average genome identity (91.8%)  
167 between these isolates than seen in other intraspecies comparisons within the family (**Figure S4**). The  
168 *E. crescens* clade is closely related to the recently proposed genus *Emergomycetes* including the *E.*  
169 *pasteurianus/africanus* species <sup>9</sup>. The *E. crescens* – *Emergomycetes* clade is a sister group of the clade  
170 including *Histoplasma* and *Blastomyces*, and *Paracoccidioides* is in a basal position for the dimorphic  
171 pathogens of the Ajellomycetaceae (**Figure 1**).

172  
173 The intercalated clades of primary pathogens (e.g. *H. capsulatum*, *P. brasiliensis* and *B. dermatitidis*),  
174 opportunistic pathogens (e.g. *E. pasteurianus*, *E. africanus*) producing a parasitic yeast phase, and  
175 non-pathogens producing adiaspore-type cells rather than yeast cells (e.g. *E. parva* and *E. crescens*)  
176 suggests that the dimorphic fungi in the Ajellomycetaceae have undergone numerous evolutionary  
177 transitions allowing adaptation, infection and virulence to humans and other mammals, and that  
178 interactions with other eukaryotes in the environment may help maintain the capacity for pathogenic  
179 growth in a mammalian host (**Figure 1**; **Table 2**). The non-thermally-dimorphic species *H. griseus* and  
180 *P. hystricis* are highly supported as early diverging lineages of Ajellomycetaceae as previously  
181 suggested <sup>13</sup>; genomic analysis strongly supports *P. hystricis* as the earliest diverging lineage within the  
182 sequenced Ajellomycetaceae, and large genetic variation between these early saprophytes. The basal  
183 position of both *H. griseus* and *P. hystricis* in the family Ajellomycetaceae and the large divergence  
184 between them suggests that the history of this family could involve evolution from saprophytic non-  
185 thermotolerant and non-yeast-forming ancestral species to dimorphic human pathogenic species after  
186 the divergence with *H. griseus*, including the adaptation to higher temperatures and the appearance of  
187 a dimorphic switch and a yeast parasitic phase (**Figure 1**).

188

### 189 **Substantial gene family contractions underlie the shift from growth on plant to animals**

190 By comparing the gene conservation and functional annotation of primary and opportunistic  
191 dimorphic pathogens with their saprophytic relatives *H. griseus* and *P. hystricis*, we identified significant  
192 decreases in gene family size (PFAM domain and GO-term counts, corrected p-value < 0.05)  
193 associated with a host/substrate shift from plants to animals in the pathogenic Ajellomycetaceae  
194 (**Figure 2**). Plant cell wall degrading enzymes are reduced in number or totally absent in dimorphic



195 pathogens compared with *H. griseus* and *P. hystricis*, including several glycosyl hydrolases, and fungal  
196 cellulose binding domain-containing proteins (**Figure 2; Table S2**). These gene family changes suggest  
197 that dimorphic fungi from Ajellomycetaceae are not typical soil fungi in that they might maintain a close  
198 association with living mammals or other organisms such as protozoa or insects. This transition  
199 appears to have occurred within the family Ajellomycetaceae after divergence from *Helicocarpus* and  
200 *Polytolypa* (**Figure 1**). Our analysis also recapitulates previous reports comparing smaller numbers of  
201 genomes from the order Onygenales<sup>5,14,17,20</sup> that showed that genes coding for enzymes involved in the  
202 deconstruction of plant cell walls were absent from all the human pathogens (e.g. *Paracoccidioides*,  
203 *Blastomyces*, *Histoplasma*, *Coccidioides*) and non-pathogenic Onygenaceae (e.g. *Uncinocarpus reesii*,  
204 *Byssoonygena ceratinophila*, *Amauroascus mutatus*, *Amauroascus niger*, *Chrysosporium*  
205 *queenslandicum*) whereas these enzymes were commonly conserved in the non-pathogens outside the  
206 order Onygenales (including *Aspergillus*, *Fusarium*, *Neurospora*; **Figure 2; Table S2**). Notably,  
207 increasing the phylogenetic density within the order Onygenales in this study revealed that the loss of  
208 plant cell wall degradative enzymes occurred independently in two families within the Onygenales, and  
209 this highlights transitions between saprophytic and pathogenic species, where *Helicocarpus* and  
210 *Polytolypa* have retained enzymes required to live on plant material in the soil, whereas non-pathogenic  
211 species from the Onygenaceae, which are not adapted to survive in mammals, have also lost capacity  
212 to degrade plant material.

213

214 Other notable changes in gene content included loss of protein families associated with secondary  
215 metabolite biosynthesis such as polyketide synthase dehydratases, and beta-ketoacyl synthases  
216 domains in dimorphic Ajellomycetaceae relative to *H. griseus* and *P. hystricis* (**Figure 2; Table S3**). We  
217 identified predicted biosynthetic clusters using the program antiSMASH (antibiotics and Secondary  
218 Metabolism Analysis Shell<sup>26</sup>). Overall, dimorphic pathogenic fungi from Ajellomycetaceae have fewer  
219 polyketide synthase (PKs) gene clusters than the saprophytic *H. griseus* and *P. hystricis* (**Table S3**;  
220 **Figure S5**). Dimorphic pathogens had lost essential genes or complete clusters of the type 1 and type  
221 3 PKs, and terpene clusters (**Table S3**). Type 3 PKs are not common in fungi, and were not previously  
222 reported in the Ajellomycetaceae. Furthermore, *H. griseus* and *P. hystricis* but not dimorphic fungi have  
223 genes related to those involved in antibiotic biosynthetic pathways (ko01055; **Table S2**). Previous  
224 studies had shown that *P. hystricis* secretes a pentacyclic triterpenoid exhibiting antifungal and  
225 antibiotic activity, denominated Polytolypin<sup>27</sup>, suggesting this terpene cluster is intact and may produce  
226 this molecule. Loss of such secondary metabolic pathways may weaken responses to other microbes in  
227 the environment. In addition to secondary metabolite biosynthesis, Ajellomycetaceae dimorphic fungi

228 showed significant decreases in pathways related with the production of sphingolipids, chloroalkane  
229 and chloroalkene degradation, linoleic acid metabolism, and bisphenol degradation (KEGG-EC counts,  
230 corrected p-value < 0.05; **Table S2**). Loss of degradative pathways for bisphenol and chloralkanes in  
231 particular likely reflect encountering these molecules in the environment but not during pathogenic  
232 growth. Altogether, these shifts in gene content highlight how the Ajellomycetaceae dimorphic  
233 pathogenic fungi became less adapted to survive in the soil than the more basally diverging saprophytic  
234 species *H. griseus* and *P. hystricis*.

### 235 236 **Transition among carbohydrate metabolism and protein catabolism**

237 We found that the evolution of carbohydrate metabolism and protein catabolism also occurred  
238 independently within the Ajellomycetaceae. We annotated carbohydrate active enzymes (CAZy) and  
239 peptidases (MEROPS; **Methods**), and using enrichment analysis found substantial shifts in the relative  
240 proportion of these groups among dimorphic and saprophytic species. Notably, the pathogenic  
241 Ajellomycetaceae species, but not the saprophytic species *H. griseus* and *P. hystricis*, showed a  
242 dramatic reduction of carbohydrate active enzymes, including 44 categories that were totally absent  
243 and 29 that were significantly depleted; these included glycoside hydrolases, glycosyltransferases,  
244 carbohydrate esterases, and polysaccharide lyases (corrected p < 0.05; **Figure 3**). The fact that these  
245 enzymes are reduced in dimorphic pathogenic Ajellomycetaceae but not in *H. griseus* and *P. hystricis*  
246 confirms that reduced carbohydrate metabolism occurred independently Ajellomycetaceae from the  
247 reduction in the Onygenaceae, originally noted in the spherule-dimorphic pathogen *Coccidioides*<sup>17</sup>. In  
248 contrast to carbohydrate active enzymes, we found that the total number of peptidases is relatively  
249 similar in dimorphic and saprophytic species within the Ajellomycetaceae. Significant protein family  
250 expansions were found to be specific in *Blastomyces*, *Histoplasma* and Onygenaceae and  
251 Arthrodermataceae species relative to *P. hystricis* and *H. griseus*, including the A11, S12, and S08A  
252 peptidases (corrected p < 0.05; **Figure 3**). The peptidase family A11 contains endopeptidases involved  
253 in the processing of polyproteins encoded by retrotransposons, and the increase in copy number is  
254 correlated with the genome expansion due to the proliferation of repetitive elements in *Blastomyces*<sup>5</sup>.  
255 The peptidase family S12 contains serine-type D-Ala-D-Ala carboxypeptidases, and S8 contains the  
256 serine endopeptidase subtilisin. Two families of fungal metalloendopeptidases (S8 and M35) were  
257 previously reported to be expanded in *Coccidioides* relative to saprophytic species outside the order  
258 Onygenales<sup>17</sup>. In addition, it has been reported that the Ajellomycetaceae includes fewer copies of  
259 multiple classes of peptidases (M36, M43, S8) as well as an associated inhibitor (I9, inhibitor of S8  
260 protease) relative to other Onygenales<sup>5</sup>. Comparing across all the Onygenales, we found that all



261 pathogenic Onygenales, as well as saprophytes related to *Coccidioides* such as *U. reesii*, had a higher  
262 ratio of proteases to carbohydrate active enzymes than the saprophytic Ajellomycetaceae *H. griseus*  
263 and *P. hystricis* (**Figure 3**). This strengthens the evidence that the adaptation and specialization of  
264 dimorphic Ajellomycetaceae occurred independently and that non-pathogenic Onygenaceae may  
265 represent an intermediate state in showing gene content changes associated with pathogens, which  
266 allowed these fungi to use proteins as a main source of energy in nutrient-limited environments.

267

268

### 269 **Loss of transporters in Ajellomycetaceae dimorphic fungi**

270 In addition to major shifts in enzymes that support nutrient acquisition, the dimorphic  
271 Ajellomycetaceae have undergone losses of families of transporters. These include the large classes of  
272 major facilitator superfamily transporters (PF07690) and sugar transporters (PF00083) (**Figure 2**). The  
273 number of transporters correlates with the numbers of genes predicted to have transmembrane helices  
274 (1,848 and 1,745 proteins have predicted transmembrane domains in *H. griseus* and *P. hystricis*,  
275 respectively, relative to an average of 1,490 in dimorphic Ajellomycetaceae pathogens, **Figure 4**). To  
276 characterize gene gain and losses in transporters, we annotated transporter families (**Methods**,<sup>28</sup>), and  
277 found significant expansion of 18 classes of transporters encompassing 9 families in *H. griseus* and *P.*  
278 *hystricis* relative to dimorphic Ajellomycetaceae pathogens (corrected *p-value* < 0.05; **Figure 4**).  
279 Transporter families that were totally absent or significantly reduced in pathogenic species included the  
280 sugar porter, anion:cation symporter, AAA-ATPase, ammonium transporter and carnitine O-Acyl  
281 transferase. The substrates of these transporters include galacturonate, Rip1, hexoses, dipeptides,  
282 allantate, ureidosuccinate, allantoin, glycerol, sulfate, sulfite, thiosulfate, sulfonates, tartrate, thiamine,  
283 cellobiose, cellodextrin, ammonia, methylamine, phenylacetate, beta-lactams, trichothecene, and  
284 carnitine O-octanoyl (**Figure 4**). Most of these compounds are only present in the plant cell wall,  
285 including the cellulose, hemicellulose, or pectin types, supporting that dimorphic pathogens have  
286 evolved to have more limited compounds from plant cell wall as source of energy.

287

### 288 **Pathogenesis-related genes are conserved in both saprophytic and pathogenic lifestyles**

289 Genes known to be important in the response to stress imposed by the host, including  
290 virulence-associated or yeast-phase specific genes of central importance in dimorphic fungi in the  
291 Onygenales, are conserved in *H. griseus* and *P. hystricis*. These include heat shock response proteins  
292 (*HSF*, *HSP90*, *HSP70*), dimorphic switch related proteins (*RYP1*, *RYP2*, *RYP3*, *AGS1*, *FKS1*),  
293 oxidative stress and hypoxia response proteins (*CATB*, *CATP*, *SOD3*, *SRB1*), as well as antigens

294 (*PbGP43*, *PbP27*, *BAD1*; **Table S4**<sup>21</sup>). In dimorphic pathogenic fungi both morphological transitions  
295 and growth temperature are linked, and loss of genes necessary for high-temperature growth and  
296 morphological transition in these pathogens results in attenuated virulence, which highlights that they  
297 are essential for pathogenesis<sup>29–31</sup>. Some of these genes such as the *RYP1*-3 transcriptional regulators  
298 and the dimorphism-regulating histidine kinase *DRK1* have been connected with morphogenetic  
299 adaptation in response to environmental stimuli, and with key determinants of the mycelia to yeast  
300 transition in dimorphic human pathogenic fungi in the Ajellomycetaceae<sup>29,30</sup>. Although *H. griseus* and  
301 *P. hystricis* are not dimorphic and cannot grow at 37 °C, the heat shock response has been shown to  
302 be highly evolutionarily conserved among eukaryotes. The fact that genes of central importance for  
303 high-temperature growth and dimorphic switch are conserved in *H. griseus* and *P. hystricis* suggests  
304 that these saprophytes may sense different gradations of temperature, or that the mechanism that  
305 triggers a rapid response to the adaptation may not be rapid enough to enable these fungi to grow at 37  
306 °C.

307

308 Dimorphic Ajellomycetaceae may have evolved specialized mechanisms to regulate their transcriptional  
309 responses; these include expansion of proteins related to the regulation of transcription, and protein  
310 kinase activity (GO term enrichment analysis;  $q$ -value < 0.05; **Table S2**), which are all expanded in  
311 dimorphic pathogens relative to *H. griseus* and *P. hystricis*. Thus, the gain of transcription factors,  
312 transcriptional regulators and phosphotransferases suggests that rapid evolution of transcriptional  
313 mechanisms may underlie the adaptation to both high temperature and the dimorphic transition. As one  
314 of the largest categories enriched in dimorphic Ajellomycetaceae but not in saprophytic species was the  
315 protein kinase activity (**Table S2**), we further classified protein kinases using Kinannotate<sup>32</sup>, including the  
316 divergent fungal-specific protein kinase (*FunK1*; **Methods**). We found an expansion of the *FunK1*  
317 family, in dimorphic Ajellomycetaceae as previously reported<sup>5,14</sup>. As we increased the phylogenetic  
318 density in the Ajellomycetaceae, including species and strains with high genetic and phenotypic  
319 variation this allowed resolution of the evolutionary history of this family of kinases (**Figure 5**). *FunK1*  
320 family is enriched in the systemic pathogens *B. dermatitidis/gilchristii*, *H. capsulatum*, *Paracoccidioides*,  
321 but limited in saprophytic species, *H. griseus* and *P. hystricis*. Notably, this family is also limited in the  
322 adiaspore-forming *E. parva* (UAMH130, UAMH139), *E. crescens* (UAMH4076) but not in *E. crescens*  
323 (UAMH3008). In addition, we found that the recently described primary pathogen *B. percursus* includes  
324 a large expansion of *FunK1* kinases, with almost twice the number as compared with its closest relative  
325 *B. dermatitidis* (**Figure 5**). Phylogenetic analysis of *FunK1* genes revealed that this family undergone

326 independent lineage-specific expansions in primary dimorphic pathogens of both Ajellomycetaceae and  
327 Onygenaceae, but not in non-pathogenic or opportunistic dimorphic species (**Figure 5**).

328

329 To identify specific genes that evolved within the Ajellomycetaceae to enable the dimorphic transition  
330 and infection of mammals, we identified and examined ortholog clusters that were unique to these  
331 pathogens and absent in both *H. griseus* and *P. hystricis*. We identified 75 ortholog clusters that were  
332 present in dimorphic Ajellomycetaceae and dimorphic Onygenaceae species but absent in *H. griseus*  
333 and *P. hystricis* (i.e. 'sporophyte gene loss events'), and 212 ortholog clusters that were present in  
334 dimorphic Ajellomycetaceae, but absent in the dimorphic Onygenaceae species, *H. griseus* and *P.*  
335 *hystricis* (i.e. 'dimorphic Ajellomycetaceae gene gain events'; **Table S5**). The gene loss events include  
336 a mold specific protein (CIMG\_00805), a phenol 2-monooxygenase (BDFG\_05966), as well as several  
337 protein kinases and transporters. The gene gain events include several protein kinases, transporters,  
338 transcription factors, and peptidases (**Table S5**). In addition, we annotated genes that have been  
339 broadly associated with host-pathogen interactions (Pathogen Host interaction database PHI), and  
340 genes that have been reported as virulence factors in fungal species (Database of Fungal Virulence  
341 Factors DFVF) <sup>33,34</sup>. We found that many genes that have been associated with host-pathogen  
342 interactions are present in the saprophytic *P. hystricis* and *H. griseus*, and in fact some appear at  
343 higher copy number counts (**Table S5**). This emphasizes that host-pathogen interaction and virulence  
344 factors are not only important for pathogenicity in mammals, but also for saprophytic species to survive  
345 and adapt to stress in the environment, including for example the ability to evade the engulfment by  
346 amoebae, or the interaction with insects <sup>35,36</sup>.

347

### 348 **Conservation of genes induced during *in vivo* infection**

349 We also hypothesized that genes induced during mammalian infection in dimorphic  
350 Ajellomycetaceae pathogens might have different gene conservation patterns among *Blastomyces*,  
351 *Histoplasma*, *Paracoccidioides*, and the novel species and saprophytes. Transcriptional responses  
352 during an *in vivo* mouse model of infection had been studied in *B. dermatitidis* (strain ATCC26189; <sup>5</sup>)  
353 and *P. brasiliensis* (strain Pb18; <sup>37</sup>). In both *B. dermatitidis* and *P. brasiliensis* the high-affinity zinc  
354 transporter, *ZRT1* (BDFG\_09159; PADG\_06417) and the flavodoxin-like protein *PST2* (BDFG\_08006;  
355 PADG\_07749) were highly induced during infection; these genes are conserved in all Ajellomycetaceae  
356 included in this analysis (**Table S6**). Of the 72 *in vivo*-induced genes in *B. dermatitidis* ATCC26188,  
357 22% are absent from the *P. hystricis* genome and 11% are absent from the *H. griseus* genome. The  
358 genes absent in *P. hystricis* include the cysteine dioxygenase (BDFG\_08059), an acetyltransferase

359 (BDFG\_07903), a thioesterase (BDFG\_02348), a superoxide dismutase (BDFG\_07895), a  
360 sodium/hydrogen exchanger (BDFG\_05427), and a response regulator protein (BDFG\_01066). In  
361 addition, we identified three secreted proteins that were found induced during the interaction of *B.*  
362 *dermatitidis* with macrophages (BDFG\_08689, BDFG\_06057, BDFG\_03876)<sup>5</sup> that are found  
363 conserved only in the dimorphic Ajellomycetaceae pathogens but not in *H. griseus*, *P. hystricis*, or  
364 outgroup species. These are strong candidates for effector proteins involved in host infection. Similar  
365 numbers of genes found induced during *in vivo* infection in *P. brasiliensis* were absent in *P. hystricis*  
366 and *H. griseus*, (23% and 17.5%, respectively; **Table S6**). Genes absent in both species include Gpr1  
367 family protein (PADG\_08695), isovaleryl-CoA dehydrogenase (PADG\_05046), glutathione-dependent  
368 formaldehyde-activating (PADG\_05832), predicted transmembrane protein (PADG\_05761), and ergot  
369 alkaloid biosynthetic protein A (PADG\_07739). Many of the genes that were absent in *P. hystricis* and  
370 *H. griseus*, were also absent in at least one of the dimorphic pathogens in the Ajellomycetaceae,  
371 highlighting species-specific gene gain events that may confer virulence specialization.

372

### 373 **Evolution of the mating type locus in the Onygenales family Ajellomycetaceae**

374 To elucidate the evolution of the mating system in the Ajellomycetaceae, we identified and  
375 characterized the mating locus of *P. hystricis*, and *H. griseus*. Notably, these two species have both  
376 mating type idiomorphs *HMG* box (*MAT 1-2*) and alpha box (*MAT1-1*); these are therefore the only  
377 homothallic species identified so far within the Ajellomycetaceae (**Figure 6**). Comparative analysis  
378 showed that the locus is not expanded relative to other Ajellomycetaceae species (21 kb between the  
379 flanking genes *SLA2* to *APN2/COX13*), unlike the expansion that observed in the larger genomes of *B.*  
380 *dermatitidis* or *B. gilchristii* (~60 kb;<sup>38</sup>). One difference is that a sequence inversion between *APN2* and  
381 *COX13* is uniquely observed in *P. hystricis* relative to all other sequenced Ajellomycetaceae species,  
382 including *H. griseus* and previously reported species<sup>5,15,38,39</sup>. This inversion observed in *P. hystricis*  
383 (mating type idiomorph flanked by *SLA2* and *APN2/COX13*) is similar to the gene order in the  
384 Onygenaceae species *Coccidioides* spp. but not in the Arthrodermataceae species *M. gypseum*  
385 (*Nannizzia gypsea*<sup>40</sup>) or *T. rubrum* (**Figure 6; Table S7**) suggesting that independent inversion events  
386 within the locus. In addition, we identified the mating type locus in non-pathogenic Onygenaceae, and  
387 found that *Amauroascus mutatus* and *Byssoonygena ceratinophila* have both mating type idiomorphs  
388 (**Table S7**). In *A. mutatus*, *HMG* box (*MAT 1-2*) and alpha box (*MAT1-1*) are linked in the same  
389 scaffold, however they are separated by 184 kb, including 65 protein-coding genes (**Figure 6**). The  
390 identification of homothallic mating loci in non-pathogenic species within both the Ajellomycetaceae and

391 the Onygenaceae suggests that there have been multiple transitions between homothallic and  
392 heterothallic sexual states in dimorphic pathogens and non-pathogenic species in the Onygenales.  
393

394 **DISCUSSION**

395

396 The evolution of the dimorphic Onygenales is characterized by multiple transitions between saprophytic  
397 and human pathogenic growth. By sequencing the genomes of two additional dimorphic adiaspore-  
398 forming species (*Emmonsia parva*, *E. crescens*) and two early diverging non-pathogenic, non-  
399 dimorphic species (*Helicocarpus griseus* and *Polytolypa hystricis*), we analyzed how changes in gene  
400 content correlate with transitions to pathogenesis. Our results establish an outer bound on the timing of  
401 two key events in the evolution of the Ajellomycetaceae; both the loss of genes involved in digesting  
402 plant cell walls and the expansion of proteases, transcriptional regulators, and protein kinases,  
403 occurred after divergence with *H. griseus*. The shift in these families was previously observed in both  
404 *Paracoccidioides* within this group and in the related *Coccidioides–Uncinocarpus* clade<sup>14,17</sup>; more  
405 recently the comparison with non-pathogenic Onygenaceae species supported previous reports of the  
406 contraction of gene families involved in digesting plant cell walls throughout the Onygenales, and of the  
407 expansion of gene families involved in digesting animal protein<sup>20</sup>. Whereas the studies on contraction  
408 of gene families involved in digesting plant cell walls addressed other fungi outside the order  
409 Onygenales, our analysis shows that *H. griseus* and *P. hystricis* did not experience such a contraction,  
410 which suggests that contractions in gene families involved in digesting plant cell walls throughout the  
411 Onygenales have occurred multiple times independently and more recently in Onygenaceae and  
412 Ajellomycetaceae families.

413

414 Since many virulence factors and dimorphic switch related proteins were also conserved in the rarely  
415 pathogenic (*Ea. parva* and *Ea. crescens*) and in the non-dimorphic Ajellomycetaceae species (*P.*  
416 *hystricis* and *H. griseus*), this suggests that these proteins could be needed not only for survival in the  
417 host, and that presence of virulence factors alone does not specify pathogenicity. In dimorphic  
418 Ajellomycetaceae other mechanisms such as gene regulation or selection may play a role in how these  
419 genes respond during distinct stimuli. In addition, it is possible that those virulence factors in mammals  
420 were also needed for the survival in the soil, for example to survive interaction with amoebae or in  
421 insects<sup>41</sup>. However, there are some virulence factors that are needed for virulence in mammals that are  
422 not necessary for virulence in other eukaryotes. For example, the alpha mating factor locus in  
423 *Cryptococcus neoformans* contributes to virulence in mice, but no difference was observed in the  
424 interaction of congenic *MAT $\alpha$*  and *MAT $\alpha$*  strains with amoebae<sup>42</sup>. While the human host is a very  
425 different habitat in comparison with soil or excrements of animals that are the most common natural



426 niche for this group of fungi, interactions with other eukaryotes in the environment likely selected for  
427 some properties that also predisposed species to become pathogenic to humans.

428

429 Selection pressures in the environment are responsible for the emergence and maintenance of traits  
430 that confer upon some soil microbes the capacity for survival in animal hosts. This is important to  
431 understand the evolution and emergence of novel pathogens. For example, *Emergomyces africanus*  
432 has recently emerged and numerous cases of novel yeast-forming species have been reported .  
433 However, *Emergomyces* species have not been found in other mammals like rodents or in the soil. In  
434 addition, *E. africanus* has a very restricted geographic distribution. Across the Onygenales, nearly all  
435 species have a high lower ratio of proteases to carbohydrate active enzymes; the exceptions are the  
436 two saprophytes *P. hystricis* and *H. griseus*, but not the saprophytes related to *Coccidioides* such as  
437 *Uncinocarpus reesii*. This genomic profile matches the results of growth assays for the non-pathogenic  
438 species *U. reesii*; this species can grow on a wide range of proteinaceous substrates but only a very  
439 limited range of carbohydrates, namely cellulose and its component glucose<sup>14</sup>. Together, these findings  
440 suggest that fungi in the Onygenales transitioned from saprophytes that digest plant materials to  
441 saprophytes that digest more limited plant materials and a wide range of animal proteins, and finally  
442 those that are major animal pathogens.

443

444 We found many of the genes with roles in the dimorphic transition and virulence are conserved in *Ea.*  
445 *parva* and *Ea. crescens*, and in saprophytic species *H. griseus* and *P. hystricis*, and we did not find  
446 larger patterns of gain of functional classes in pathogenic species. However, we found smaller changes  
447 in gene content related to the regulation of gene expression and signaling that may account for the  
448 ability to grow at high temperature, species specific morphological transitions, and therefore their  
449 differences in virulence, since rapid thermo-tolerance and morphological adaptation is essential for  
450 pathogenesis<sup>29,30,43</sup>. Overall, we found significant expansions of the number of the protein kinase  
451 *FunK1* family, transcription factors and other genes associated with the regulation of gene expression  
452 in yeast-forming Ajellomycetaceae relative to adiaspore-forming and saprophytic species. Our  
453 comparison with saprophytic Ajellomycetaceae highlights dramatic decreases and complete absences  
454 of several classes of gene families that are important for survival and growth in a soil environment.

455

456 Intriguingly, we found that both more basal non-pathogenic Ajellomycetaceae species *H. griseus* and *P.*  
457 *hystricis* appear homothallic, in striking contrast to all the previously described largely pathogenic  
458 species in this group that are all heterothallic. *P. hystricis* has a fused mating type locus, with both

459 idiomorphs, *HMG* box (*MAT 1-2*) and alpha box (*MAT1-1*), fused at a single locus, and the same is  
460 likely true of *H. griseus*, as genes are located at the ends of two scaffolds in this assembly. In addition,  
461 we found that this is also true for the non-pathogenic Onygenaceae species *Amauroascus mutatus* and  
462 *Byssoonygena ceratinophila*; these species have both mating type idiomorphs. *A. mutatus* has both  
463 mating type idiomorphs located on the same scaffold; however, these are separated by a much larger  
464 distance than is typically observed at the *MAT* locus of homothallic fungi. This suggests that this locus  
465 has been subject to recombination events either to bring the two idiomorphs nearby on the same  
466 scaffold or alternatively in expansion of a fused locus. While it has been previously suggested that the  
467 ancestor of the Onygenales very likely was heterothallic<sup>39</sup>, the placement of multiple lineages of  
468 homothallic species in this group raises the possibility of a heterothallic ancestor, with more recent  
469 transitions in pathogenic species to be homothallic and rearrangements of the mating locus in others  
470 such as *P. hystericis* and *A. mutatus*. Both *P. hystericis* UAMH7299 and *H. griseus* UAMH5409 can  
471 develop ascomata and ascospores, which have been shown to sporulate in *P. hystericis*<sup>11,27,44</sup>. Loss of  
472 the capacity for homothallic self-mating could increase the frequency of out-crossing and this may be  
473 beneficial to some species under pressure from their environment or host<sup>45</sup> such as the pathogenic  
474 species in this group. Examining the mating type loci of additional non-pathogenic species in the  
475 Onygenales would further reveal if there are novel configurations of homothallic or heterothallic loci,  
476 which may help infer the mating ability of ancestral species and the timing of transitions in pathogens  
477 and non-pathogens.

478  
479 Our phylogenomic analysis revealed that dimorphic pathogens in the Onygenales have undergone  
480 multiple evolutionary transitions that enabled infection of humans and other mammals. Some such as  
481 the loss of plant cell wall degrading enzymes are convergent for pathogens in the two families of  
482 Onygenales. Our comparisons also revealed major differences in non-pathogenic species between  
483 these two families, which suggested that some species appear intermediate between saprophytes and  
484 pathogens in terms of having a shift in metabolic capacity without associated pathogenic growth.  
485 Targeting additional intermediate species within the Ajellomycetaceae with different phenotypes (e.g.  
486 *Emmonsiiellopsis*) for genome sequencing and comparison would help further refine the picture of the  
487 overall evolution of this important group of fungi.

488

## 489 MATERIALS AND METHODS

490

### 491 Genome sequencing

492 Species were selected for sequencing based on previous estimates of high genetic variation  
493 among the members of the genus *Emmonsia*, especially in the *E. parva* species, and based on  
494 observations of the emergence of *Emmonsia*-like species in the Ajellomycetaceae causing systemic  
495 human mycoses worldwide<sup>8,9</sup>. We selected one strain of *Emmonsia parva* (UAMH130; CBS139881;  
496 type strain) and one additional strain of *Emmonsia crescens* (UAMH4076; CBS139868). *E. parva*  
497 UAMH130 is from the lungs of a rodent in the USA, and *E. crescens* UAMH4076 is from a greenhouse  
498 source in Canada, and mated with *E. crescens* UAMH129, 349<sup>22</sup>. In addition, the first strictly non-  
499 pathogenic non-dimorphic species from the Ajellomycetaceae, one strain of *Helicocarpus griseus*  
500 (UAMH5409; a.k.a. *Spiromastix grisea*) and *Polytolypa hystricis* (UAMH7299) were selected for whole  
501 genome sequencing. Genomic DNA was isolated from mycelial phase at 22 °C. We constructed one  
502 library with 180-base inserts and sequenced on the Illumina HiSeq 2000 platform to generate 101 bp  
503 paired-end reads with high coverage (173X UAMH4076; 199X UAMH130; 205X UAMH5409; 163X  
504 UAMH7299).

505

### 506 Genome assembly, gene prediction and annotation

507 The 101-bp Illumina reads of *E. parva* UAMH130, *E. crescens* UAMH4076, *P. hystricis* and *H.*  
508 *griseus* were assembled using ALLPATHS-LG<sup>46</sup> with default parameters. All four *de novo* assemblies  
509 were evaluated using the GAEMR package (<http://software.broadinstitute.org/software/gaemr/>), which  
510 revealed no aberrant regions of coverage, GC content or contigs with sequence similarity suggestive of  
511 contamination. Scaffolds representing the mitochondrial genome were separated out from the nuclear  
512 assembly.

513

514 Genes were predicted and annotated by combining calls from multiple methods to obtain the best  
515 consensus model for a given locus. These included *ab initio* predictions (GlimmerHMM, Augustus,  
516 Snap, GeneMark-ES), homologous inference (Genewise, TBLastN), and gene model consolidation  
517 programs (EvidenceModeler)<sup>47,48</sup>. For the protein coding-gene name assignment we combined  
518 HMMER PFAM/TIGRFAM, Swissprot and Kegg products. Kinanote was used to annotate protein  
519 kinases<sup>32</sup>. To evaluate the completeness of predicted gene sets, the representation of core eukaryotic  
520 genes was analyzed using CEGMA genes<sup>23</sup> and BUSCO<sup>24</sup>.

521

## 522 Identification of orthologs and phylogenomic analysis

523 To compare gene content and conservation, we identified orthologous gene clusters in these  
524 sequenced genomes and in other Onygenales genomes using OrthoMCL (version 1.4) with a Markov  
525 in a on index of 1.5 and a maximum e-value of  $1e-5$ <sup>49</sup>. We included the genomes of the classical  
526 dimorphic pathogenic species (*Blastomyces dermatitidis*, *B. gilchristii*, *Histoplasma capsulatum*,  
527 *Paracoccidioides brasiliensis*, *P. lutzii*, *Coccidioides immitis*, and *C. posadasii*), novel dimorphic human  
528 pathogenic species (*Blastomyces percursus*, *Emergomyces africanus*, *E. pasteurianus*), and two  
529 dimorphic non-human pathogenic species *Emmonsia parva* UAMH139 and *Emmonsia crescens*, along  
530 with other species, including three *Aspergillus* (**Table S1**; **Figure S7**). In addition, we annotated and  
531 included in the compare gene content and conservation analysis the available genomes of saprophytic  
532 species from the family Onygenaceae *Byssoonygena ceratinophila* (UAMH5669), *Amauroascus*  
533 *mutatus* (UAMH3576), *Amauroascus niger* (UAMH3544), and *Chrysosporium queenslandicum*  
534 (CBS280.77), and the genome of the yeast-forming dimorphic pathogen *Emergomyces orientalis*  
535 (5Z489, **Table S1**). Although, this is the largest genomic data set of Ajellomycetaceae strains so far, the  
536 number of shared gene families after each addition of genome data did not clearly reach a plateau; this  
537 suggests that the current estimate of a core of 4,200 genes is too high, and that more genomes are  
538 needed to define the core-genome and pan-genome in the Ajellomycetaceae (**Figure S6**).

539  
540 To examine the phylogenetic relationship of the newly sequenced *E. parva* and *E. crescens*, *P. hystricis*  
541 and *H. griseus* relative to other dimorphic fungi we used single copy orthologs determined and  
542 clustered using OrthoMCL. A total of 31 genomes from the Onygenales order and three *Aspergillus*  
543 genomes were chosen to estimate the species phylogeny (**Table S1**). These include the four newly  
544 strains described here: *E. parva* UAMH130, *E. crescens* UAMH4076, *P. hystricis* UAMH7299 and *H.*  
545 *griseus* UAMH5409, as well as the following: three *Blastomyces dermatitidis* (ATCC26199,  
546 ATCC18188, ER-3), one *Blastomyces gilchristii* (SLH14081), one *Emmonsia parva* (UAMH139), one  
547 *Emmonsia crescens* (UAMH3008), two *Histoplasma* (WU24, G186AR), five *Paracoccidioides* (Pb01,  
548 Pb03, Pb18, PbCnh, Pb300), two *Coccidioides* (RS, Silveira), *Uncinocarpus reesii* (UAMH1704),  
549 *Microsporium gypseum* (CBS118893), *Trichophyton rubrum* (CBS118892), *Aspergillus nidulans* (FGSC  
550 A4), *A. flavus* (NRRL3357) and *A. fumigatus* (Af293). Protein sequences were aligned using MUSCLE,  
551 and a phylogeny was estimated from the concatenated alignments using RAxML v7.7.8<sup>50</sup> with model  
552 PROTCATWAG with a total of 1,000 bootstrap replicates.

553

## 554 Gene family and protein domain analysis

555 To identify gene content changes that could play a role in the evolution of the dimorphism and  
556 pathogenesis within Ajellomycetaceae, we searched for expansions or contractions in functionally  
557 classified genes compared to the other fungi from the order Onygenales. Genes were functionally  
558 annotated by assigning PFAM domains, GO terms, and KEGG classification. HMMER3<sup>51</sup> was used to  
559 identify PFAM domains using release 27. GO terms were assigned using Blast2GO<sup>52</sup>, with a minimum  
560 e-value of  $1 \times 10^{-10}$ . Protein kinases were identified using Kinannoter<sup>32</sup> and divergent FunK1 kinases  
561 were further identified using HMMER3. We further annotated carbohydrate active enzymes, peptidases,  
562 and transporter families using the CAZY version 07-15-2016<sup>53</sup>, MEROPS version 9.12<sup>54</sup>, and TCDB  
563 version 01-05-2017<sup>28</sup> databases, respectively. Proteins were searched against their corresponding  
564 databases using BLAST, with minimum e-values of  $1 \times 10^{-80}$  for CAZY,  $1 \times 10^{-20}$  for MEROPS, and  
565  $1 \times 10^{-20}$  for TCDB.

566

567 To identify functional enrichments in the compared genomes, we used four gene classifications:  
568 OrthoMCL similarity clusters, PFAM domains, KEGG pathways, and Gene Ontology (GO), including  
569 different hierarchy levels, MEROPS and CAZY categories, and transporter families. Using a matrix of  
570 gene class counts for each classification type, we identified enrichment comparing two subsets of  
571 queried genomes using Fisher's exact test. Fisher's exact test was used to detect enrichment of PFAM,  
572 KEGG, GO terms, CAZY, MEROPS, and transporter families between groups of interest, and p-values  
573 were corrected for multiple comparisons<sup>55</sup>. Significant (corrected p-value < 0.05) gene class  
574 expansions or depletions were examined for different comparisons.

575

#### 576 **Data Availability Statement**

577 The raw sequences, genome assemblies and gene annotations were deposited in GenBank under the  
578 following BioProject accession numbers: *Emmonsia parva* strain UAMH130 (PRJNA252752),  
579 *Emmonsia crescens* strain UAMH4076 (PRJNA252751), *Polytolypa hystricis* strain UAMH7299  
580 (PRJNA234736), and *Helicocarpus griseus* strain UAMH5409 (PRJNA234735).

581

582 **ACKNOWLEDGEMENTS**

583 We thank Lynne Sigler for her help in selecting strains for sequencing. We thank the Broad Genomics  
584 Platform for generating Illumina sequence for this study, Sarah Young and Margaret Priest for their  
585 assistance in assembly and annotation, Christopher Desjardins for helpful comments on the  
586 manuscript, and Leslie Gaffney for help with Figure 1. This project has been funded in whole or in part  
587 with Federal funds from the National Institute of Allergy and Infectious Diseases, National Institutes of  
588 Health, Department of Health and Human Services, under award N°: U19AI110818. This work was  
589 partly supported by Colciencias via the grants under Contract N°: 122256934875 and N°:  
590 221365842971, and by the Universidad de Antioquia via a “Sostenibilidad 2016” grant.

591

592 **Author contributions**

593 Conceived and designed the experiments: JFM JGM OKC CAC. Performed the assembly and  
594 annotation: JFM CAC. Analyzed the data: JFM CAC. Contributed reagents/materials/analysis tools:  
595 JGM OKC. Wrote the paper: JFM CAC.

596

597 **Additional information**

598 Competing interests: The authors declare no competing financial interests.

599

600



601 **Tables and Figures**

602

603 **Table 1.** Statistics of the annotated genome assemblies of *Emmonsia*, *Helicocarpus* and *Polytolypa*

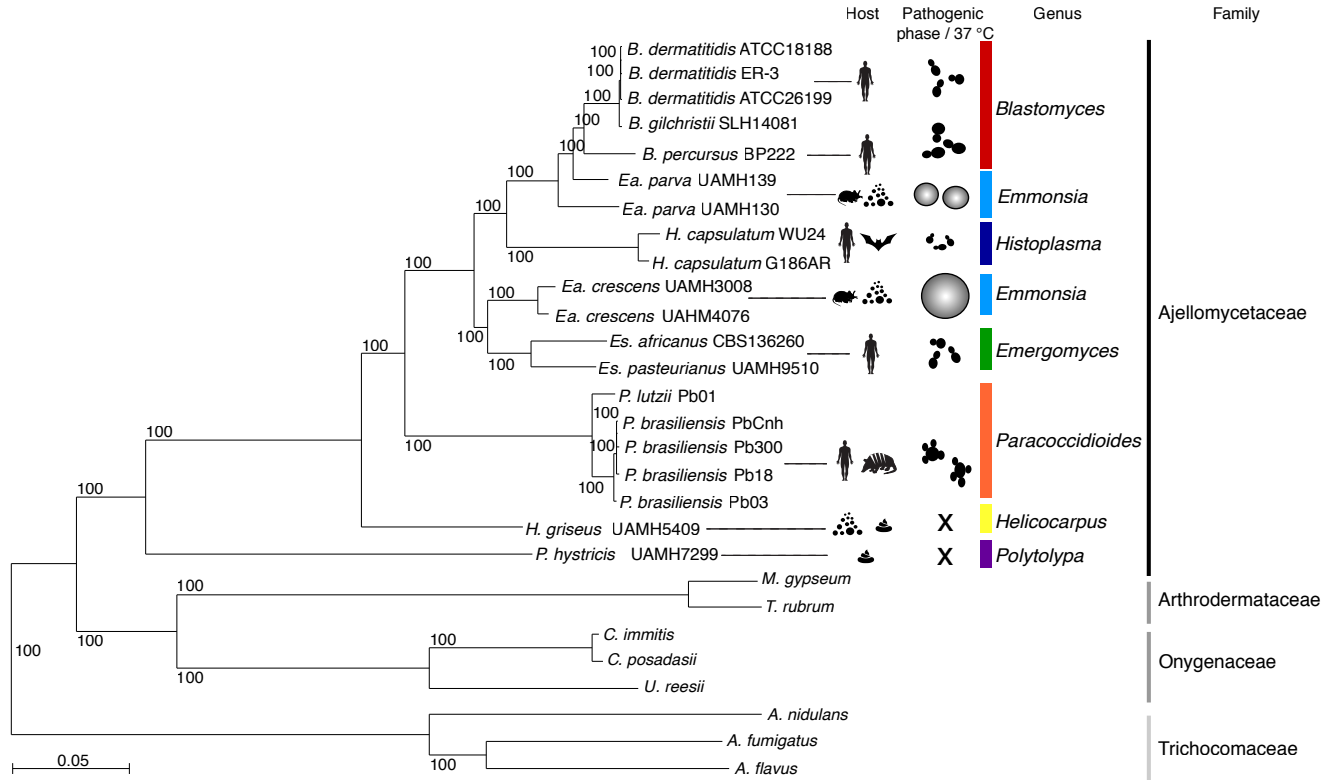
Species	Strain	Assembly (Mb)	Scaffolds (count)	N50 (kb)	GC (%)	Repeat (%)	Genes (count)
<i>Emmonsia parva</i>	UAMH130	27.8	383	173.2	47.5	2.6	8,202
<i>Emmonsia crescens</i>	UAMH4076	33.8	1,288	96.6	42.9	15.0	8,909
<i>Helicocarpus griseus</i>	UAMH5409	34.7	641	135.7	48.0	1.8	10,225
<i>Polytolypa hystricis</i>	UAMH7299	32.0	546	124.6	45.6	12.8	9,935

604

605 **Table 2.** Thermo-dimorphic pathogenic fungi, expansion and diversity within Ajellomycetaceae

Species	Family	Dimorphism	Parasitic phase	Virulence in human
<i>Blastomyces gilchristii</i>	Ajellomycetaceae	Yes	Intermediate yeast	Primary pathogen
<i>Blastomyces dermatitidis</i>	Ajellomycetaceae	Yes	Intermediate yeast	Primary pathogen
<i>Blastomyces persicus</i>	Ajellomycetaceae	Yes	Large yeast	Primary pathogen
<i>Emmonsia parva</i>	Ajellomycetaceae	Yes	Small adiaspore	Occasional
<i>Histoplasma capsulatum</i>	Ajellomycetaceae	Yes	Small yeast	Primary pathogen
<i>Emmonsia crescens</i>	Ajellomycetaceae	Yes	Large adiaspore	Occasional
<i>Emergomyces pasteurianus</i>	Ajellomycetaceae	Yes	Small yeast	Opportunistic
<i>Emergomyces africanus</i>	Ajellomycetaceae	Yes	Small yeast	Opportunistic
<i>Paracoccidioides brasiliensis</i>	Ajellomycetaceae	Yes	Multibudding yeast	Primary pathogen
<i>Paracoccidioides lutzii</i>	Ajellomycetaceae	Yes	Multibudding yeast	Primary pathogen
<i>Lacazia loboi</i>	Ajellomycetaceae	ND	Multibudding yeast	Primary pathogen
<i>Helicocarpus griseus</i>	Ajellomycetaceae	No	No	Non-pathogen
<i>Polytolypa hystricis</i>	Ajellomycetaceae	No	No	Non-pathogen
<i>Coccidioides immitis</i>	Onygenaceae	Yes	Spherules	Primary pathogen
<i>Coccidioides posadasii</i>	Onygenaceae	Yes	Spherules	Primary pathogen
<i>Sporothrix schenckii</i>	Ophiostomataceae	Yes	Small yeast	Primary pathogen
<i>Talaromyces marneffeii</i>	Trichocomaceae	Yes	Small septate yeast	Primary pathogen

606



607

608

**Figure 1. Phylogenomic relationships and diversity in the family Ajellomycetaceae.** Maximum

609

likelihood phylogeny (2,505 core genes based on 1,000 replicates) including 20 annotated genome

610

assemblies of species within the family Ajellomycetaceae, five other Onygenales and three *Aspergilli*.

611

All nodes were supported by 100% of bootstrap replicates. Color bars indicate the genus and icons

612

represent most common source or host. Illustrations of the most common morphology at 37 °C or in the

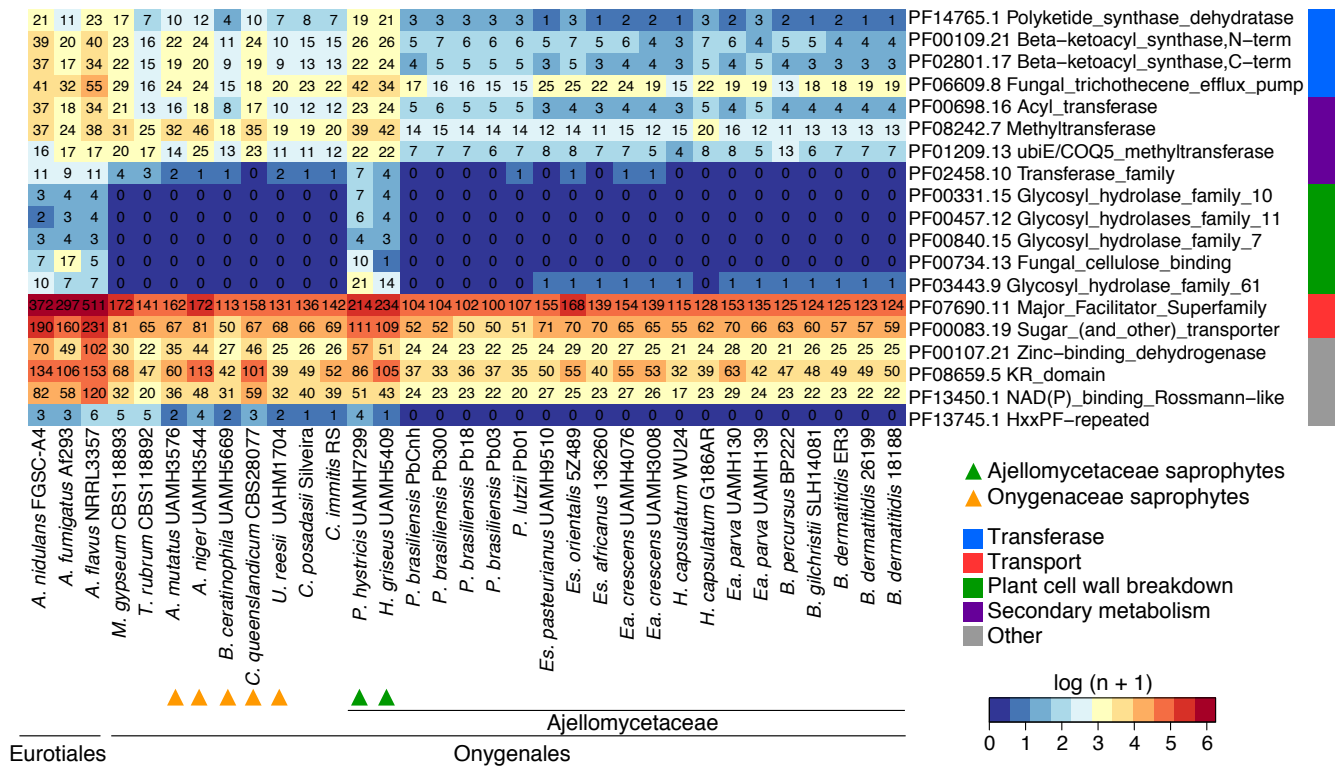
613

host are depicted for selected species highlighting the phenotypic variation within the Ajellomycetaceae

614

and the transition to human hosts represented by pathogenicity traits.

615



616

617

618

619

620

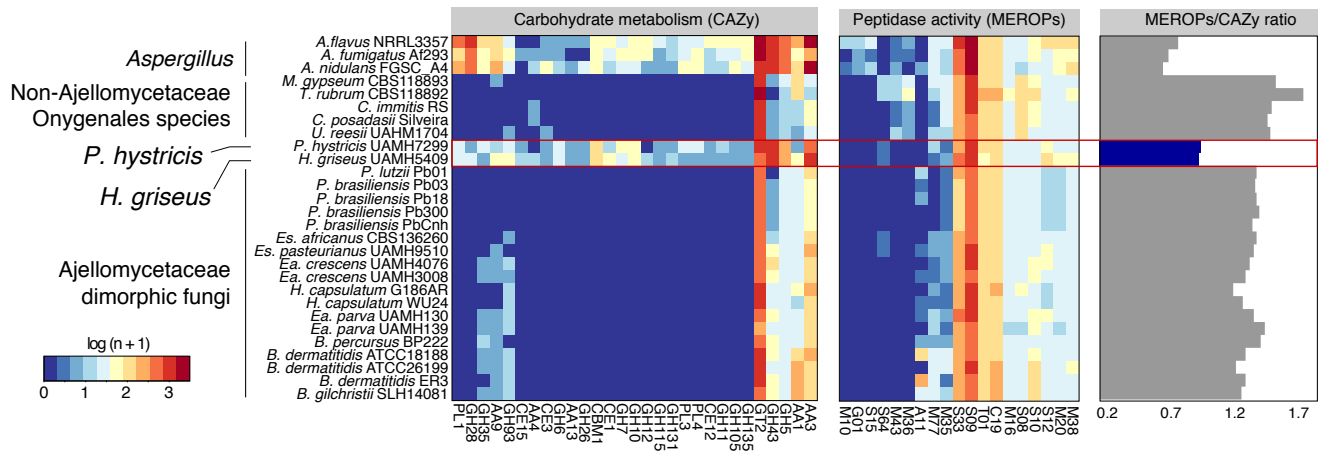
621

622

623

624

625



626

627

**Figure 3. Shifts in carbohydrate metabolism and peptidase activity in Ajellomycetaceae.**

628

Heatmaps depicting for each taxon carbohydrate metabolism categories (CAZy) and peptidase families

629

(MEROPs) across the Ajellomycetaceae species included in this study and other compared genomes.

630

These categories were found significantly enriched (corrected  $p$ -value < 0.05) in the non-dimorphic

631

systemic fungi *P. hystricis* and *H. griseus* relative to Ajellomycetaceae dimorphic fungi, or within

632

Ajellomycetaceae species and other compared genomes from Onygenaceae and Arthrodermataceae

633

families, or Eurotiales order. The ratio of MEROPS genes to CAZY genes for each genome across the

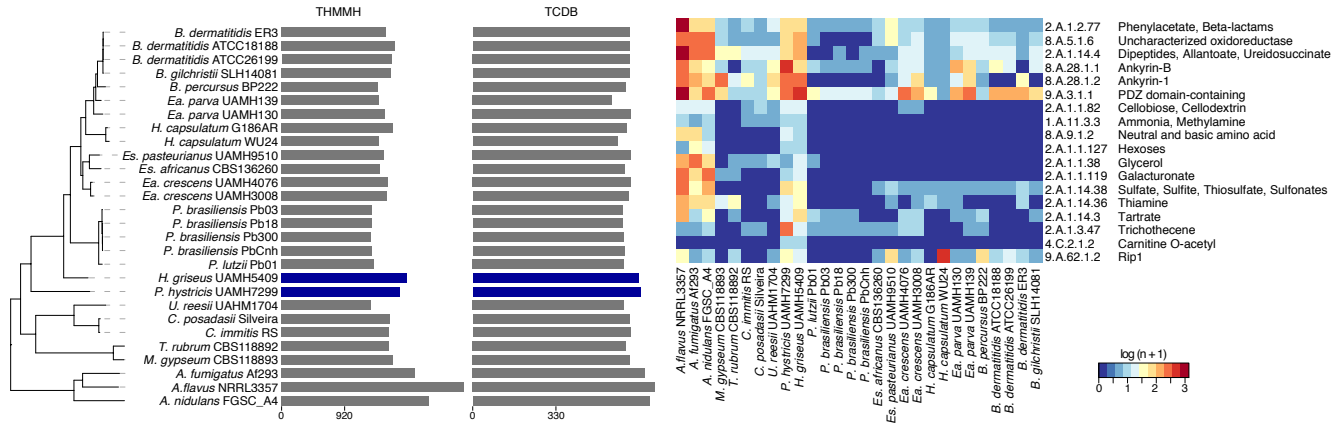
634

Ajellomycetaceae species included in this study and other compared genomes is shown at right.

635

*Es: Emergomyces; Ea: Emmonsia.*

636



637

638

**Figure 4. Shifts in metabolism matched substrate preference within Ajellomycetaceae**

639

**contraction of transporters within the Ajellomycetaceae.** (right) Heatmap depicting the number of

640

family transporters (TCDB; color-code blue: low, red: high) for each taxon across the Ajellomycetaceae

641

species and other compared genomes. These families were found significantly enriched (test, corrected

642

*p-value* < 0.05) in the non-dimorphic *P. hystricis* and *H. griseus* relative to dimorphic Ajellomycetaceae

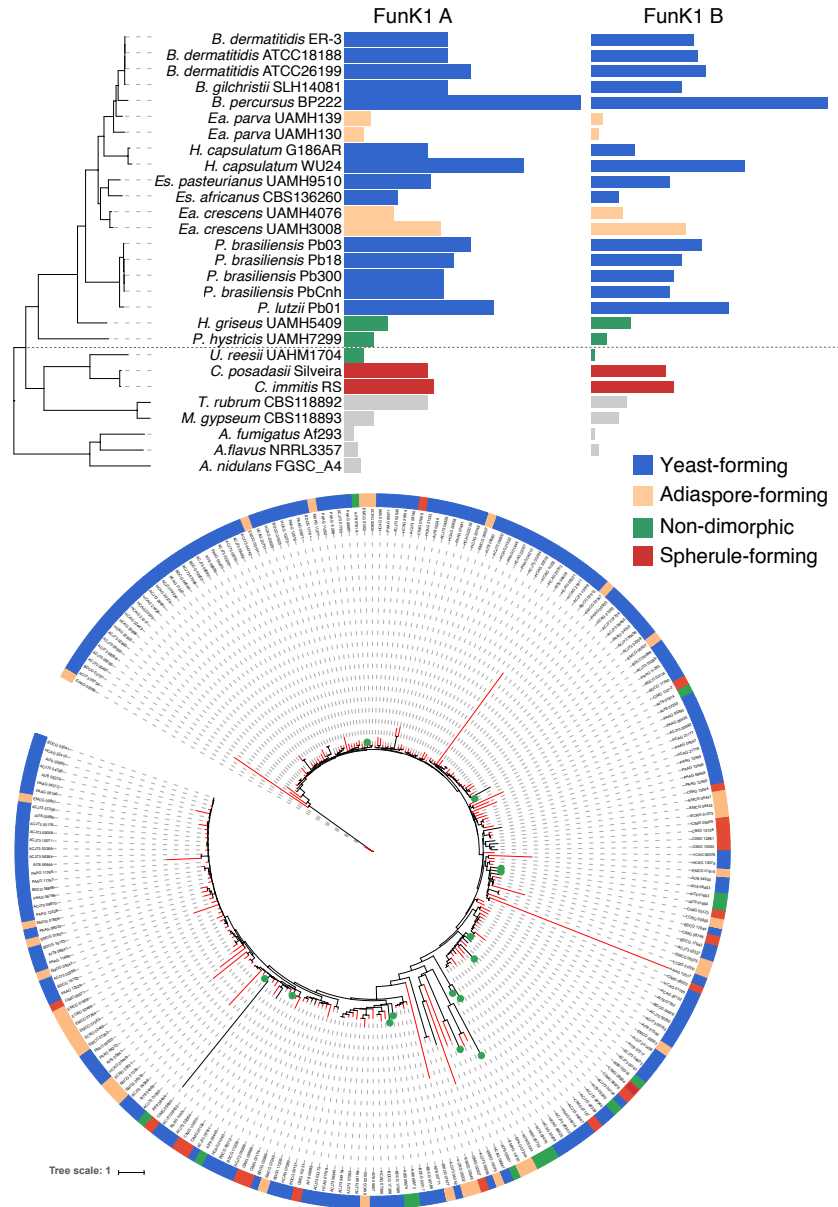
643

fungi. (left) Total number of transporters identified in the genomes for each taxon included in this study.

644

*Es:* *Emergomyces*; *Ea:* *Emmonsia*.

645

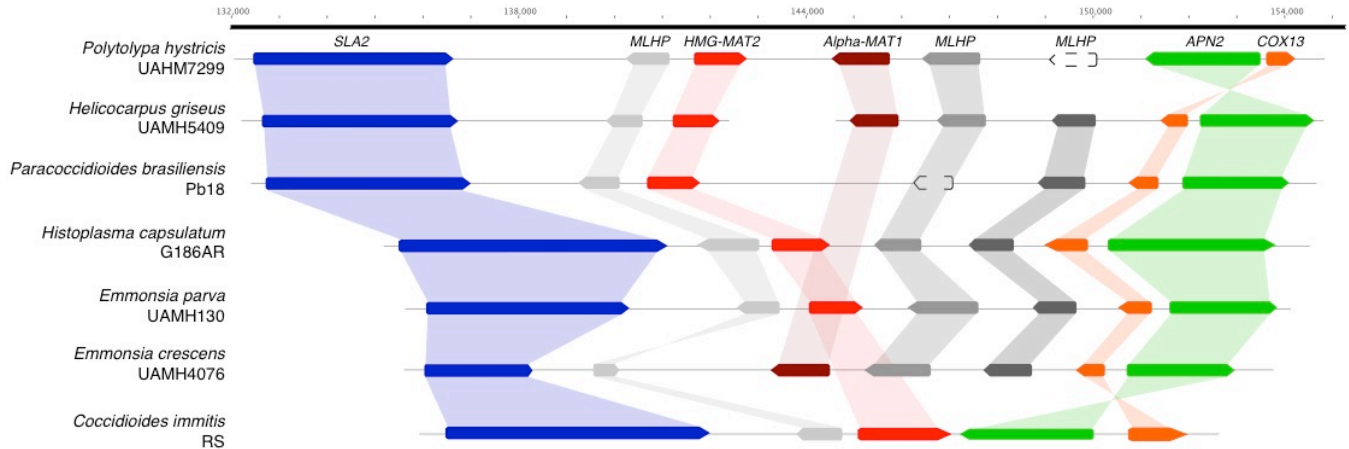


646

647 **Figure 5. Expansion and contraction of protein kinases class *FunK1* across the**  
 648 **Ajellomycetaceae.** (top) *FunK1 A* and *FunK1 B* counts for each taxon across the Ajellomycetaceae  
 649 species and other compared genomes. The tree shown corresponds to the maximum likelihood  
 650 phylogenetic tree of the family Ajellomycetaceae from Fig. 1. (bottom) Maximum likelihood tree of  
 651 *FunK1* family showing expansion in Ajellomycetaceae yeast-forming (blue) pathogenic species. Each  
 652 species (top) or gene (bottom) has a color code indicating the parasitic phase at 37 °C (yeast,  
 653 adiaspore, spherule, or non-pathogenic).

654





655

656

**Figure 6. Mating type evolution within the Onygenales family Ajellomycetaceae.** (top) Synteny  
657 synteny schema depicting orientation and conservation of the genes adjacent to the mating type locus  
658 idiormorphs HMG box (*MAT 1-2*, red) and alpha box (*MAT1-1*, dark red) in the Ajellomycetaceae. The  
659 more basal species, *P. hystricis*, has both mating type idiormorphs intact, being the only homothallic  
660 species identified so far within the Ajellomycetaceae. The locus has similar size to other  
661 Ajellomycetaceae species with 21 kb average from *SLA2* (blue) to *APN2/COX13* (green/orange), but  
662 not *Blastomyces dermatitidis/gilchristii* (60 kb; Li W et al., 2013). A synteny inversion encompassing  
663 *APN2* and *COX13* is uniquely observed in this ancestor relative to the rest of Ajellomycetaceae species  
664 included in this study, including *H. griseus*. Grey genes are mating locus hypothetical proteins (MLHP).

665

666 **References**

667

- 668 1. Klein, B. S. & Tebbets, B. Dimorphism and virulence in fungi. *Curr Opin Microbiol* **10**, 314–9  
669 (2007).
- 670 2. Sil, A. & Andrianopoulos, A. Thermally dimorphic human fungal pathogens--Polyphyletic  
671 pathogens with a convergent pathogenicity trait. *Cold Spring Harb Perspect Med* **5**, a019794  
672 (2015).
- 673 3. Gauthier, G. M. Dimorphism in fungal pathogens of mammals, plants, and insects. *PLoS Pathog*  
674 **11**, e1004608 (2015).
- 675 4. England, D. M. & Hochholzer, L. Adiaspiromycosis: an unusual fungal infection of the lung.  
676 Report of 11 cases. *Am J Surg Pathol* **17**, 876–86 (1993).
- 677 5. Munoz, J. F. *et al.* The dynamic genome and transcriptome of the human fungal pathogen  
678 *Blastomyces* and close relative *Emmonsia*. *PLoS Genet* **11**, e1005493 (2015).
- 679 6. Herr, R. A. *et al.* Phylogenetic analysis of *Lacazia loboi* places this previously uncharacterized  
680 pathogen within the dimorphic Onygenales. *J Clin Microbiol* **39**, 309–14 (2001).
- 681 7. Kenyon, C. *et al.* A dimorphic fungus causing disseminated infection in South Africa. *N Engl J*  
682 *Med* **369**, 1416–1424 (2013).
- 683 8. Schwartz, I. S. *et al.* 50 Years of *Emmonsia* disease in humans: the dramatic emergence of a  
684 cluster of novel fungal pathogens. *PLoS Pathog* **11**, e1005198 (2015).
- 685 9. Dukik, K. *et al.* Novel taxa of thermally dimorphic systemic pathogens in the Ajellomycetaceae  
686 (Onygenales). *Mycoses* **60**, 296–309 (2017).
- 687 10. Wang, O. *et al.* A novel dimorphic pathogen, *Emergomycetes orientalis* (Onygenales), agent of  
688 disseminated infection. *Mycoses* (**in press**), (2017).
- 689 11. Marin-Felix, Y. *et al.* *Emmonsiellopsis*, a new genus related to the thermally dimorphic fungi of  
690 the family Ajellomycetaceae. *Mycoses* **58**, 451–60 (2015).
- 691 12. Untereiner, W. A. *et al.* The Ajellomycetaceae, a new family of vertebrate-associated  
692 Onygenales. *Mycologia* **96**, 812–821 (2004).
- 693 13. Untereiner, W. A., Scott, J. A., Naveau, F. A., Currah, R. S. & Bachewich, J. Phylogeny of  
694 *Ajellomyces*, *Polytolypa* and *Spiromastix* (Onygenaceae) inferred from rDNA sequence and  
695 non-molecular data. *Stud Mycol* **47**, 25–35 (2002).
- 696 14. Desjardins, C. A. *et al.* Comparative genomic analysis of human fungal pathogens causing  
697 paracoccidioidomycosis. *PLoS Genet* **7**, e1002345 (2011).
- 698 15. Munoz, J. F. *et al.* Genome diversity, recombination, and virulence across the major lineages of  
699 *Paracoccidioides*. *mSphere* **1**, (2016).
- 700 16. Neafsey, D. E. *et al.* Population genomic sequencing of *Coccidioides* fungi reveals recent  
701 hybridization and transposon control. *Genome Res* **20**, 938–46 (2010).
- 702 17. Sharpton, T. J. *et al.* Comparative genomic analyses of the human fungal pathogens  
703 *Coccidioides* and their relatives. *Genome Res* **19**, 1722–31 (2009).
- 704 18. Burmester, A. *et al.* Comparative and functional genomics provide insights into the pathogenicity  
705 of dermatophytic fungi. *Genome Biol* **12**, R7 (2011).
- 706 19. Martinez, D. A. *et al.* Comparative genome analysis of *Trichophyton rubrum* and related  
707 dermatophytes reveals candidate genes involved in infection. *MBio* **3**, e00259-12 (2012).
- 708 20. Whiston, E. & Taylor, J. W. Comparative phylogenomics of pathogenic and nonpathogenic  
709 species. *G3 Bethesda* **6**, 235–44 (2015).
- 710 21. Munoz, J. F. *et al.* Genome update of the dimorphic human pathogenic fungi causing  
711 paracoccidioidomycosis. *PLoS Negl Trop Dis* **8**, e3348 (2014).

- 712 22. Sigler, L. *Ajellomyces crescens* sp. nov., taxonomy of *Emmonsia* spp., and relatedness with  
713 *Blastomyces dermatitidis* (teleomorph *Ajellomyces dermatitidis*). *J Med Vet Mycol* **34**, 303–14  
714 (1996).
- 715 23. Parra, G., Bradnam, K. & Korf, I. CEGMA: a pipeline to accurately annotate core genes in  
716 eukaryotic genomes. *Bioinformatics* **23**, 1061–7 (2007).
- 717 24. Simão, F. A., Waterhouse, R. M., Ioannidis, P., Kriventseva, E. V. & Zdobnov, E. M. BUSCO:  
718 assessing genome assembly and annotation completeness with single-copy orthologs.  
719 *Bioinformatics* **31**, 3210–3212 (2015).
- 720 25. Peterson, S. W. & Sigler, L. Molecular genetic variation in *Emmonsia crescens* and *Emmonsia*  
721 *parva*, etiologic agents of adiaspiromycosis, and their phylogenetic relationship to *Blastomyces*  
722 *dermatitidis* (*Ajellomyces dermatitidis*) and other systemic fungal pathogens. *J Clin Microbiol* **36**,  
723 2918–25 (1998).
- 724 26. Blin, K. *et al.* antiSMASH 4.0—improvements in chemistry prediction and gene cluster boundary  
725 identification. *Nucleic Acids Res.* **45**, W36–W41 (2017).
- 726 27. Gamble, W. R., Gloer, J. B., Scott, J. A. & Malloch, D. Polytolypin, a new antifungal triterpenoid  
727 from the coprophilous fungus *Polytolypa hystricis*. *J. Nat. Prod.* **58**, 1983–1986 (1995).
- 728 28. Saier, M. H., Jr., Tran, C. V. & Barabote, R. D. TCDB: the Transporter Classification Database  
729 for membrane transport protein analyses and information. *Nucleic Acids Res* **34**, D181-6 (2006).
- 730 29. Beyhan, S., Gutierrez, M., Voorhies, M. & Sil, A. A temperature-responsive network links cell  
731 shape and virulence traits in a primary fungal pathogen. *PLoS Biol* **11**, e1001614 (2013).
- 732 30. Nemecek, J. C., Wuthrich, M. & Klein, B. S. Global control of dimorphism and virulence in fungi.  
733 *Science* **312**, 583–8 (2006).
- 734 31. Rappleye, C. A., Eissenberg, L. G. & Goldman, W. E. *Histoplasma capsulatum* alpha-(1,3)-  
735 glucan blocks innate immune recognition by the beta-glucan receptor. *Proc Natl Acad Sci USA*  
736 **104**, 1366–1370 (2007).
- 737 32. Goldberg, J. M. *et al.* Kinannoter, a computer program to identify and classify members of the  
738 eukaryotic protein kinase superfamily. *Bioinformatics* **29**, 2387–94 (2013).
- 739 33. Lu, T., Yao, B. & Zhang, C. DFVF: database of fungal virulence factors. *Database J. Biol.*  
740 *Databases Curation* **2012**, (2012).
- 741 34. Winnenburg, R. *et al.* PHI-base: a new database for pathogen host interactions. *Nucleic Acids*  
742 *Res.* **34**, D459–D464 (2006).
- 743 35. Casadevall, A., Steenbergen, J. N. & Nosanchuk, J. D. `Ready made' virulence and `dual use'  
744 virulence factors in pathogenic environmental fungi—the *Cryptococcus neoformans* paradigm.  
745 *Curr Opin Microbiol* **6**, 332–337 (2003).
- 746 36. Derengowski Lda, S. *et al.* The transcriptional response of *Cryptococcus neoformans* to  
747 ingestion by *Acanthamoeba castellanii* and macrophages provides insights into the evolutionary  
748 adaptation to the mammalian host. *Eukaryot Cell* **12**, 761–74 (2013).
- 749 37. Pigosso, L. L. *et al.* *Paracoccidioides brasiliensis* presents metabolic reprogramming and  
750 secretes a serine proteinase during murine infection. *Virulence* **0**, 1–18 (2017).
- 751 38. Li, W. *et al.* Identification of the mating-type (MAT) locus that controls sexual reproduction of  
752 *Blastomyces dermatitidis*. *Eukaryot Cell* **12**, 109–17 (2013).
- 753 39. Li, W., Metin, B., White, T. C. & Heitman, J. Organization and evolutionary trajectory of the  
754 mating type (MAT) locus in dermatophyte and dimorphic fungal pathogens. *Eukaryot Cell* **9**, 46–  
755 58 (2010).
- 756 40. Hoog, G. S. de *et al.* Toward a novel multilocus phylogenetic taxonomy for the dermatophytes.  
757 *Mycopathologia* **182**, 5–31 (2017).
- 758 41. Steenbergen, J. N., Shuman, H. A. & Casadevall, A. *Cryptococcus neoformans* interactions with  
759 amoebae suggest an explanation for its virulence and intracellular pathogenic strategy in  
760 macrophages. *Proc. Natl. Acad. Sci.* **98**, 15245–15250 (2001).

- 761 42. Nielsen, K. *et al.* *Cryptococcus neoformans*  $\alpha$  strains preferentially disseminate to the central  
762 nervous system during coinfection. *Infect. Immun.* **73**, 4922–4933 (2005).
- 763 43. Rappleye, C. A. & Goldman, W. E. Defining virulence genes in the dimorphic fungi. *Annu Rev*  
764 *Microbiol* **60**, 281–303 (2006).
- 765 44. Sugiyama, M., Ohara, A. & Mikawa, T. Molecular phylogeny of onygenalean fungi based on  
766 small subunit ribosomal DNA (SSU rDNA) sequences. *Mycoscience* **40**, 251–258 (1999).
- 767 45. Heitman, J., Sun, S. & James, T. Y. Evolution of fungal sexual reproduction. *Mycologia* **105**, 1–  
768 27 (2013).
- 769 46. Gnerre, S. *et al.* High-quality draft assemblies of mammalian genomes from massively parallel  
770 sequence data. *Proc Natl Acad Sci U A* **108**, 1513–8 (2011).
- 771 47. Haas, B. J., Zeng, Q., Pearson, M. D., Cuomo, C. A. & Wortman, J. R. Approaches to Fungal  
772 Genome Annotation. *Mycology* **2**, 118–141 (2011).
- 773 48. Haas, B. J. *et al.* Automated eukaryotic gene structure annotation using EVIDENCEModeler and  
774 the Program to Assemble Spliced Alignments. *Genome Biol* **9**, R7 (2008).
- 775 49. Li, L., Stoeckert, C. J., Jr. & Roos, D. S. OrthoMCL: identification of ortholog groups for  
776 eukaryotic genomes. *Genome Res* **13**, 2178–89 (2003).
- 777 50. Stamatakis, A. RAxML-VI-HPC: maximum likelihood-based phylogenetic analyses with  
778 thousands of taxa and mixed models. *Bioinformatics* **22**, 2688–90 (2006).
- 779 51. Eddy, S. R. Accelerated Profile HMM Searches. *PLoS Comput Biol* **7**, e1002195 (2011).
- 780 52. Conesa, A. *et al.* Blast2GO: a universal tool for annotation, visualization and analysis in  
781 functional genomics research. *Bioinformatics* **21**, 3674–6 (2005).
- 782 53. Cantarel, B. L. *et al.* The Carbohydrate-Active EnZymes database (CAZy): an expert resource  
783 for glycomics. *Nucleic Acids Res* **37**, D233-8 (2009).
- 784 54. Rawlings, N. D., Barrett, A. J. & Bateman, A. MEROPS: the peptidase database. *Nucleic Acids*  
785 *Res* **38**, D227-33 (2010).
- 786 55. Storey, J. D. & Tibshirani, R. Statistical significance for genomewide studies. *Proc Natl Acad Sci*  
787 *U A* **100**, 9440–5 (2003).
- 788
- 789